J Therm Anal Calorim (2009) 96:705–713
DOI 10.1007/s10973-009-0039-y

Latent catalytic systems for ring-opening metathesis-based thermosets

T. C. Mauldin · M. R. Kessler

Received: 16 September 2008 / Accepted: 28 April 2009 / Published online: 10 June 2009

Abstract Synthesis and curing activity of latent ring-opening metathesis polymerization (ROMP)-based catalytic systems are reported using polydicyclopentadiene (pDCPD) as a model system. Differential scanning calorimetry (DSC) is used to monitor the ROMP reactions and to characterize the cured networks. These systems are either slow or completely inactive at ambient temperatures, yet at high temperatures the superior curing activity of other ROMP catalysts are retained. The resulting thermosets show glass transition temperatures from 10 to 25 °C higher than when cured with other ROMP catalysts.

Keywords Curing kinetics · Grubbs catalysts · Ozawa–Flynn–Wall isoconversional model-free approach · Ring-opening metathesis polymerization

Introduction

Thermosets made via ring-opening metathesis polymerization (ROMP) [1, 2] are commercially available under the trade names Telene®, Metton®, and Vestenamer®, among others, and they generally are lightweight, possess high glass transition temperatures and have high impact strengths. These commercial systems are made with early transition metal-based catalysts such as tungsten, molybdenum or tantalum [3–5], all of which provide processing problems owing to their air-instability, variable curing activity, and occasional requirement of solvent. In the last several years, however, a series of air-stable, functional group tolerant, and highly active ruthenium ROMP catalysts have been developed, but they are not yet widely used for commercial applications. These ruthenium catalysts, often dubbed "Grubbs' catalysts," [6–9] show promise in developing ROMP thermosets, but probably fall short of requirements for prepreg resins or for reaction injection molding (RIM) due to their extremely high activity, even at sub-ambient temperatures.

In this study, we develop two novel Grubbs'-type catalytic systems that demonstrate latent curing behavior at low temperatures while retaining the high activity of other ruthenium-based catalysts at elevated temperatures. The first system consists of a catalyst designed to inherently disfavor initiation of polymerization, therefore requiring higher temperatures, and the second system uses the commercially available 2nd generation Grubbs' catalyst [10] along with additives that externally inhibit ligand dissociation. The monomer dicyclopentadiene (DCPD) is used as a model system, and the kinetics of its cure is studied by differential scanning calorimetry and analyzed further using the Ozawa–Flynn–Wall isoconversional model-free approach.

Experimental

Materials

Trimethylphosphine and all solvents were purchased from Aldrich and, unless otherwise specified, used without further purification. Grubbs' 2nd generation catalyst, $(IMesH_2)(P\text{-}Cy_3)(Cl)_2Ru(=CHPh)$ **1** (Fig. 2), was lyophilized according

T. C. Mauldin
Department of Chemistry, Iowa State University, Ames, IA 50011, USA

M. R. Kessler (✉)
Department of Materials Science and Engineering, Iowa State University, 2220 Hoover Hall, Ames, IA 50011, USA
e-mail: mkessler@iastate.edu

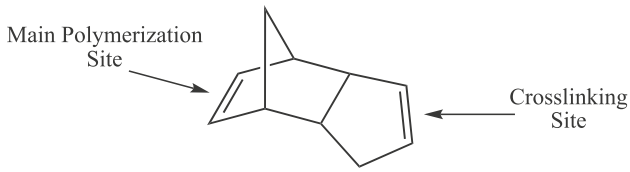

Fig. 1 Chemical structure of dicyclopentadiene (DCPD)

to the literature [11] to assist its solubility. Dicyclopentadiene (>95% *endo*-isomer) was purchased from Alpha Aesar, and the chemical structure is shown in Fig. 1.

$$(H_2IMes)(PMe_3)(Cl)_2Ru(=CHPh) \quad (3)$$

Complex **2** was synthesized according to the literature [12], and its manipulation was performed using standard Schlenk techniques under an atmosphere of dry nitrogen gas. Complex **3** was synthesized by a modified procedure in the literature [13]. To a solution of complex **2** (20 mg, 0.0275 mmol) dissolved in 2 ml dry benzene was added trimethylphosphine (4.18 mg, 0.055 mmol), and the reaction mixture was stirred for 10 min. The solvent was evaporated in vacuo, washed with cold pentanes (4 × 5 ml), and dried under vacuum for 2 h to yield a brown powder (13.5 mg, 76% yield), shown in Fig. 2. 1H NMR ($CDCl_3$): δ 19.06 (s, 1H, = C*H*Ph), 7.90 (d, J = 7.5 Hz, 2H, ortho C*H*), 7.47 (t, J = 7.5 Hz, 1H, para C*H*), 7.16 (t, J = 7.5 Hz, 2H, meta C*H*), 7.00 (s, 2H, Mes C*H*), 6.40 (s, 2H, Mes C*H*), 4.10 (m, 4H, NCH_2CH_2 N), 2.64 (s, 6H, ortho CH_3), 2.37 (s, 6H, ortho CH_3), 2.31 (s, 3H, para CH_3), 2.02 (s, 3H, para CH_3), 0.90 (d, J = 9.6 Hz, 9H, PCH_3). Anal. Calcd. For $C_{31}H_{41}N_2Cl_2PRu$: C, 57.76%; H, 6.42%; N, 4.34%. Found: C, 57.95%; H, 6.51%; N, 4.11%.

General DSC technique

Dicyclopentadiene, used either neat or containing dissolved triphenylphosphine, was added to the ruthenium-based ROMP catalyst, stirred quickly until complete catalyst dissolution, and flash-frozen in liquid nitrogen. The resulting solid was slightly melted to remove sample for experiments and refrozen in liquid nitrogen between tests. Samples were loaded into a DSC (Model Q20, TA Instruments) at a standby temperature of −50 °C. DSC experiments for all catalyst systems were under a flow of nitrogen at a constant rate of 50 ml/min. Dynamic curing experiments were performed over a temperature range of −50–200 °C at heating rates of 3, 7, 10, 15, and 20 °C/min.

Isoconversional model-free approach

Degree of cure (α) measured by differential scanning calorimetry is defined as the fraction of heat or enthalpy at a given time:

$$\alpha = \Delta H_t / \Delta H_{rxn} \quad (1)$$

where ΔH_t is the heat evolved at time t and ΔH_{rxn} is the total heat evolution during the curing process. Curing kinetics can then be modeled using the typical curing equation

$$\delta\alpha/\delta t = k(T)f(\alpha) \quad (2)$$

that includes reaction model $f(\alpha)$ and the temperature-dependant rate constant $k(T)$. The latter can be further expanded

$$k = A\ e^{(Ea/RT)} \quad (3)$$

to reveal the activation parameters A (pre-exponential factor) and E_a (activation energy). The isoconversional model-free approach assumes that both of these activation parameters are a function of degree of cure (α), and they can be calculated by performing dynamic DSC scans and monitoring how the temperature to reach different degrees of cure changes with different heating rates. To achieve this, Ozawa [14] and Flynn and Wall [15] developed an approach by which Eq. 2 is integrated, and the resulting integral partially solved to give an equation of the form:

$$\ln\beta = -1.052(E_a/RT_i) + C \quad (4)$$

where β is the heating rate, T_i is the temperature required to reach a specific conversion, and C is a combination of other terms, including the pre-exponential factor (A). At a given conversion i, a plot of ln β vs. $1/T_i$ over all heating rates then yields a straight line with a slope proportional to E_a.

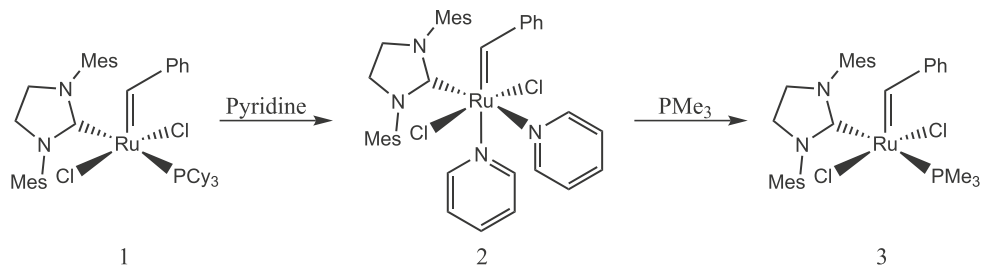

Fig. 2 Synthetic route to latent catalyst **3**

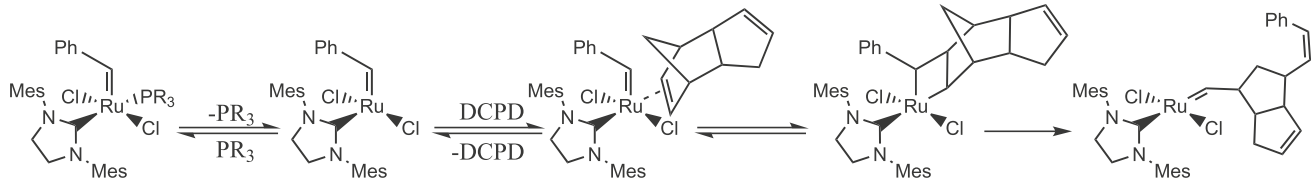

Fig. 3 ROMP of dicyclopentadiene by a 2nd generation Grubbs'-type catalyst

Results and discussion

The mechanism for ring-opening metathesis polymerization of dicyclopentadiene with a ruthenium complex is shown in Fig. 3. DCPD first replaces the phosphine via dissociative substitution, followed by rearrangement of electrons between the coordinated olefin and carbene to form the metallocyclobutane intermediate, and finally a similar rearrangement of electrons to open the ring and add a penultimate unit to the polymer chain. This gives rise to a new carbene with a neighboring open coordination site to which another monomer can bind and further propagate the growing active chain end. The fact that the only ligands known to be labile on Grubbs'-type catalysts are the phosphine, and their dissociation is necessary for the catalyst to activate and begin propagating, allows this dissociation to be considered an initiation step while the remainder of the catalytic cycle is propagation. This bodes well for designing catalysts with a long pot-life since the degree of latency should be tunable by varying the phosphine moiety in order to inhibit initiation at lower temperatures. Intuitively, these catalysts with various different phosphines should preserve the high catalytic activity of 2nd generation Grubbs' catalyst **1** since the propagating metal species, sans phosphine, are identical.

Complex **3** was synthesized by indirectly replacing the PCy_3 ligand in complex **1** with PMe_3 (Fig. 2). As shown in Fig. 4, curing of dicyclopentadiene with complex **3** is

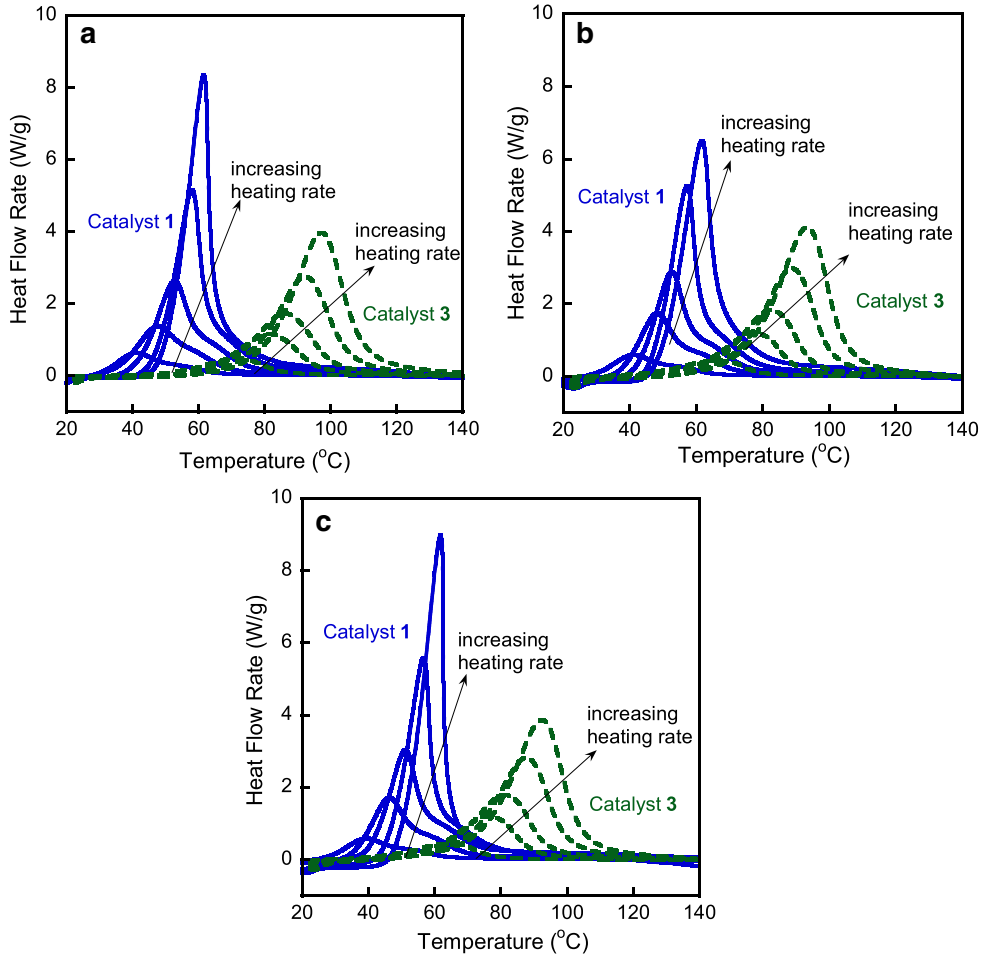

Fig. 4 DSC curves of samples with **a** 4000:1, **b** 3000:1, and **c** 2000:1 molar ratio of [DCPD]:[catalyst] for catalysts **1** (*solid line*) and **3** (*dashed line*) at five different heating rates: 3, 7, 10, 15, and 20 °C/min

clearly more latent than with complex **1** at various mole % loadings of each catalyst.

The degree of latency for the two catalysts is well-explained by the electronic and steric parameters of their respective phosphines. Electronically, the more nucleophilic a ligand, the slower dissociation tends to be. Ligands that act as strong nucleophiles have a high affinity for electrophiles like transition metals, and the bonds formed generally have high bond strengths that require a significant input of energy to break. Also, smaller ligands are typically known to have slower dissociation kinetics. Larger ligands maximize steric congestion on the metal center, and reduction of this steric strain via dissociation helps to facilitate the dissociation process. Smaller ligands, however, do not have such a driving force and, from an enthalpic standpoint, are favored to remain coordinated to the metal.

Table 1 shows that the conjugate acid of PCy_3 has a pKa (a common measure of electronic character of phosphines) making it slightly more nucleophilic than PMe_3, which would imply that from an electronic standpoint PCy_3 is more latent. However the size of PMe_3, expressed by its cone angle, is significantly smaller than PCy_3. Seeing as catalyst **3** is considerably more latent than catalyst **1**, it appears that this greatly reduced size of PMe_3 offsets the minor electronic advantage towards latency that PCy_3 would be expected to have. Considerable effort in the literature dedicated to studying other Grubbs'-type metathesis catalysts has shown a wide range of solution phosphine dissociation rates by varying the phosphine used [16], which suggests that the curing latency of these systems can also be so tuned.

The second approach investigated to improve the latency of Grubbs'-type ROMP catalysts is by addition of free phosphine to the monomer. Figure 5 shows dynamic DSC scans of catalyst **1** with neat DCPD and catalyst **1** with 30, 60, and 120 molar equivalents (relative to catalyst) of PPh_3 initially dissolved in the DCPD. Analysis of the DSC plots confirms that addition of triphenylphosphine also inhibits dissociation of complex **1**, and the extent of the shift in the DSC curves appears proportional to the amount of free phosphine added.

This improved latency is attributed to Grubbs'-type catalysts dissociation existing in equilibrium with their respective dissociated species (Fig. 6). Addition of a large excess of free phosphine to the curing system pushes this equilibrium towards the ROMP-inactive precatalyst and increase the latency of the system. It seems that only at elevated temperatures is this equilibrium pushed towards the ROMP-active dissociated complex where appreciable amounts of reaction can occur.

Another hypothesis to explain these results is degradation of the ruthenium catalyst, facilitated by free phosphine, which has been reported elsewhere [17, 18]. This would render much catalyst inactive and effectively reduce its concentration which could, in theory, increase latency. However, our results (vide infra, Fig. 7) show that the degree of latency of catalyst **1** seems somewhat indiscriminate of catalyst loading, but very sensitive to amount of free phosphine. Hence, the latter hypothesis is not given much weight here, but the potential for a combination of both effects can not be ignored.

A comparison of the three catalyst system's peak temperatures (T_p) and temperatures at 10% cure ($T_{\alpha=0.1}$) are shown in Fig. 7. While measurement of onset temperatures for each system would probably be the best approach to quantitatively evaluate the latency of each system, comparisons are often difficult owing to the different curvature in their DSC plots. However, it is believed that a comparison of two points of reference—peak temperatures and temperatures at a low degree of cure—should at least provide some insight into the degree of latency for each system.

The difference between data sets containing 30 and 60 equivalents of free phosphine is small, but both T_p and $T_{\alpha=0.1}$ are consistently higher with 60 eq. PPh_3. Addition of 120 equivalents gives temperatures that are clearly higher over all heating rates. Since the same catalyst concentration was used in all experiments where free PPh_3 was added, it is reasonable to claim that addition of free phosphine can act as a means to "fine tune" the latency of ROMP-based systems. This trend is also in good agreement with the above argument of phosphine dissociation occurring in an equilibrium—the more free phosphine initially added, the further the equilibrium will be pushed towards the ROMP-inactive pre-catalyst, consequently requiring higher temperatures to shift the equilibrium towards the ROMP-active catalyst. The exact dependency of this latency on free phosphine loading, however, is not very clear. The difference in the T_p and $T_{\alpha=0.1}$ values between data sets containing 30 and 60 equivalents of free phosphine ranges from 1.0 to 1.5 °C over all heating rates, and the range of differences between systems containing 60 and 120 equivalents of free phosphine is 3.7–4.4 °C. This seems like a consistent trend, but the difference in T_p and $T_{\alpha=0.1}$ between data sets containing 0 and 30 equivalents of free phosphine (the data set represented by 3000:1 [DCPD]:[catalyst **1**], ○ in Fig. 7, can also be considered as a 3000:1:0 molar ratio of

Table 1 pKa and cone angle of phosphines in catalysts **1** and **3**

Phosphine	Cone angle	pKa
PCy_3	170°	9.7
PMe_3	118°	8.65
PPh_3	145	2.73

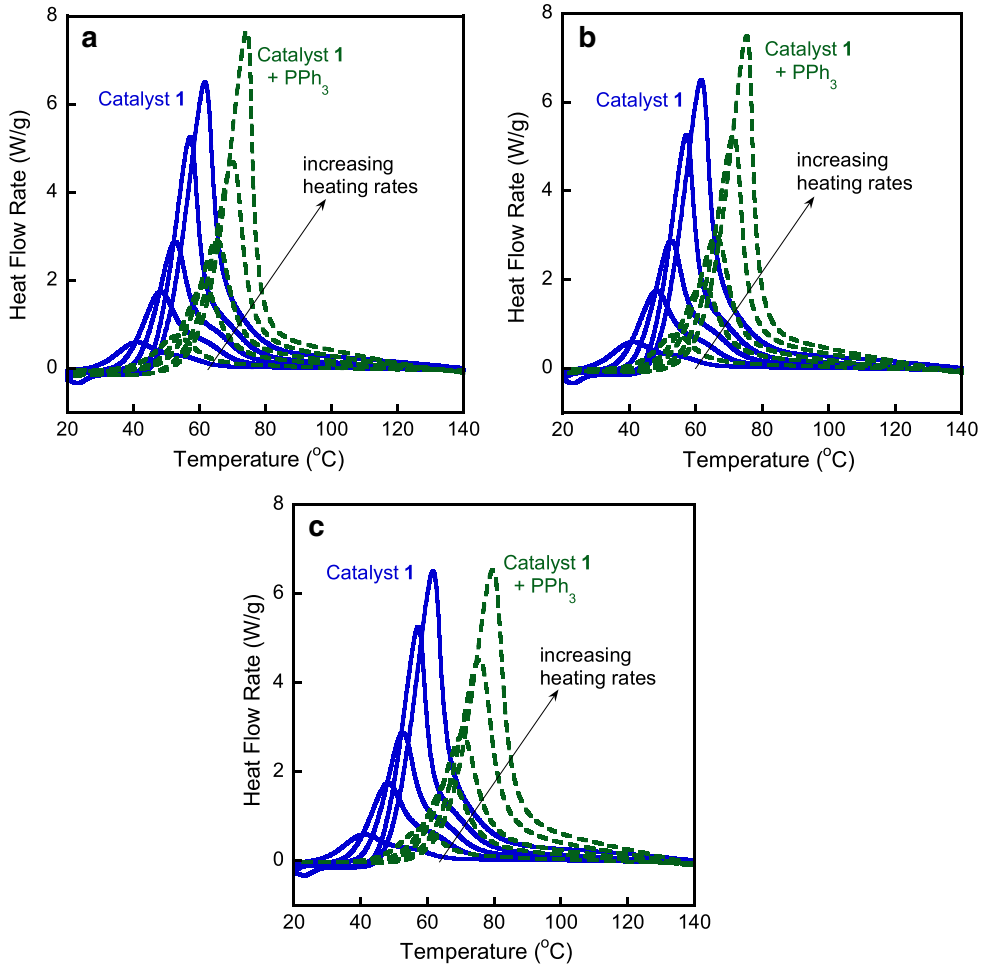

Fig. 5 DSC curves of samples with a 3000:1 molar ratio of [DCPD]:[catalyst **1**] (*solid line*) and **a** 3000:1:30, **b** 3000:1:60, and **c** 3000:1:120 molar ratio of [DCPD]:[catalyst **1**]:[PPh_3] (*dashed line*) at five different heating rates: 3, 7, 10, 15, and 20 °C/min

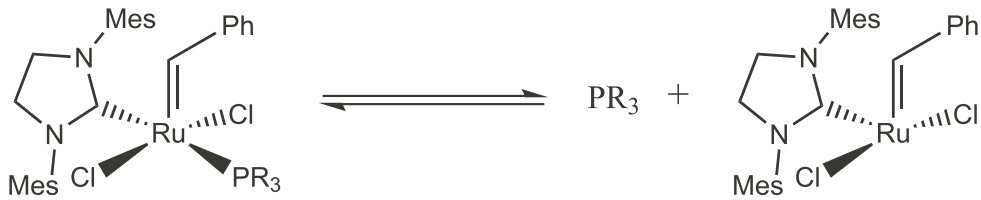

Fig. 6 Equilibrium of phosphine dissociation

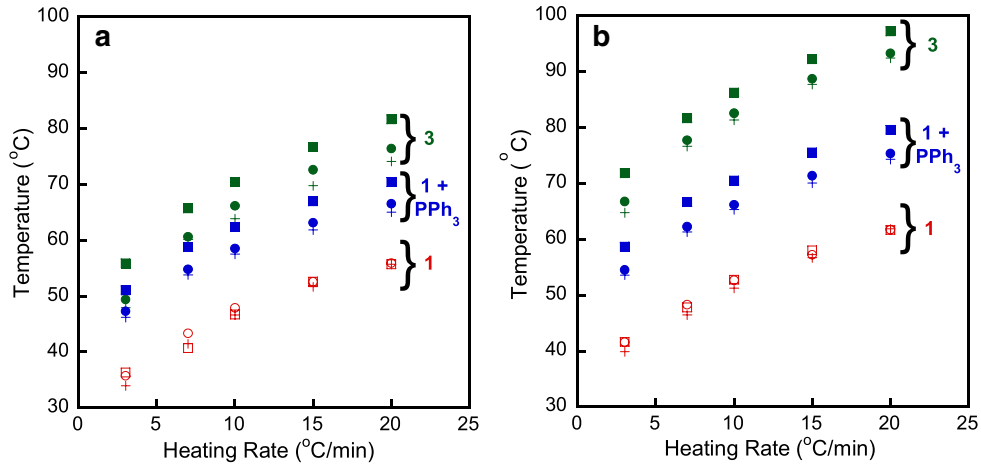

Fig. 7 **a** Temperatures at 10% cure ($T_{\alpha=0.1}$) and **b** peak temperatures (T_p) for all catalyst systems. Both plots contain data using catalyst **1** (2000:1 +, 3000:1 ○, and 4000:1 □ molar ratio [DCPD]:[Ru]), catalyst **3** (2000:1 +, 3000:1 ●, and 4000:1 ■ molar ratio [DCPD]:[Ru]), and catalyst **1** + PPh_3 (3000:1:30 +, 3000:1:60 ●, and 3000:1:120 ■ molar ratio [DCPD]:[Ru]:[PPh_3])

[DCPD]:[catalyst **1**]:[PPh_3]) is anomalously large—they range from 9.2 to 13.0 °C. A conclusive theory has not yet been formulated to explain this phenomenon, but it may be the aforementioned possibility of free phosphine both degrading catalyst, therefore reducing effective catalyst concentration and increasing latency, and existing in the equilibrium represented in Fig. 6, also increasing latency. Both effects may be active in increasing latency when small amounts of free phosphine are added until perhaps a maximum amount of catalyst degradation is reached, and the trend between data sets including 30, 60 and 120 equivalents of free phosphine is solely representative of the equilibrium in Fig. 6.

Exothermic peaks from reaction with catalyst **3** shows shifts to higher temperatures with decreasing catalyst loading. At all heating rates, the highest catalyst loading, 2000:1 [DCPD]:[catalyst], clearly have the lowest T_p and $T_{\alpha=0.1}$ values, followed by 3000:1, then 4000:1. With a higher amount of catalyst, relative to monomer, there are more polymer chains propagating at any time, and a given degree of cure can be achieved at lower temperatures. This trend is generally expected and has been observed for many different systems [X. Sheng, pers. comm.]. Catalyst **1** may show a similar trend, but it is not as apparent as with catalyst **3**. While some data points in Fig. 7 show no dependency of the exothermic peak's position on catalyst loading, most seem to follow the same trend as catalyst **3**. However, since all T_p and $T_{\alpha=0.1}$ values at each heating rate are very similar, this apparent trend cannot be conclusively distinguished from experimental error. In either case, it is at least evident that the dependency of the position of the exothermic peak is more sensitive to catalyst loading with catalyst **3** than with catalyst **1**.

Another note of interest is the material properties of the resulting polymer formed from each catalyst system. The typical glass transition temperatures, T_g, of each system is shown in Table 2. Catalyst **1** and catalyst **3** form polymers with very similar glass transition temperatures, consistently around 160 °C and 164 °C, respectively. These T_g values are considerably higher than that reported for commercial pDCPD systems of about 140–150 °C [19], most likely because the more active catalysts **1** and **3** are able to polymerize more of the less-reactive crosslinking sites on DCPD (Fig. 1) than other catalysts. Polymers made from catalyst **1** + PPh_3 have drastically reduced T_g's that drop with a higher loading of free phosphine. In samples made with catalyst **1** + PPh_3, a reduced glass transition temperature is expected, since the large amount of free phosphine can act as a plasticizer in the polymer matrix. Also presented in Table 2 is the ΔH_{rxn} for all of the catalyst systems, evaluated by taking the integral under the DSC peak corresponding to exothermic reaction. All T_g and ΔH_{rxn} values presented are very consistent and repeatable, implying that their differences are not a result of experimental error. Reasons for these differences are discussed in detail below.

Table 2 Representative glass transition temperatures (T_g) and reaction enthalpys (ΔH_{rxn}) for polymers formed from different catalyst systems

Catalyst system	T_g (°C)	ΔH_{rxn} (J/g)
1	160.3	342.3 ± 7.2
3	164.1	311.0 ± 7.7
1 + 30 eq. PPh_3	145.3	351.8 ± 2.4
1 + 60 eq. PPh_3	139.7	347.8 ± 4.8
1 + 120 eq. PPh_3	121.2	336.8 ± 3.9

Glass transition temperatures presented here were taken from samples cured at $\beta = 15$ °C/min, and T_g values were measured at a heating rate of $\beta = 15$ °C/min

The propagation of each catalyst system ideally should retain the high catalytic activity known for the 2nd generation Grubbs' catalyst [20, 21], so the dynamic scans were examined via an Ozawa–Flynn–Wall analysis to determine activation energies. This data is shown in Fig. 8.

Activation energy seems to be independent of catalyst concentration, and the general shape of the plots for all three systems shows typical diffusion control—activation energy stays relatively constant at low conversions, followed by what appears to be an exponential increase, presumably near or after the gel point. This behavior has been observed in other ROMP curing studies [22]. Assuming the nearly constant activation energy at low degrees of cure is the best representation of the propagation activity of each catalyst, it appears that both catalyst **1** and catalyst **3** have similar propagation activity, within experimental error. This effect is expected, considering both catalysts have the same propagating metal center.

The higher activation energy at low conversions for the system containing catalyst **1** + PPh_3 probably results directly from the equilibrium shown in Fig. 6. Even at higher temperatures when the equilibrium is expected to favor the ROMP-active species, the mere presence of at most 120 equivalents of free phosphine should be statistically likely to rebind with some propagating catalyst molecules, forcing them back into their dormant, precatalyst state. The aggregate energy required to both activate the polymerization and to frequently re-dissociate phosphine from the catalyst is then expected to be higher than the other systems.

Figure 8a and b, activation energy profiles for catalysts **1** and **3**, respectively, show similar activation energies at conversions from 0 to 0.3 and 0.9. From 0.4 to 0.8, however, the two plots deviate significantly. All best-fit lines in the plots of ln β vs. $1/T_i$, from which Fig. 8 was derived, were good fits to the experimental data with correlation

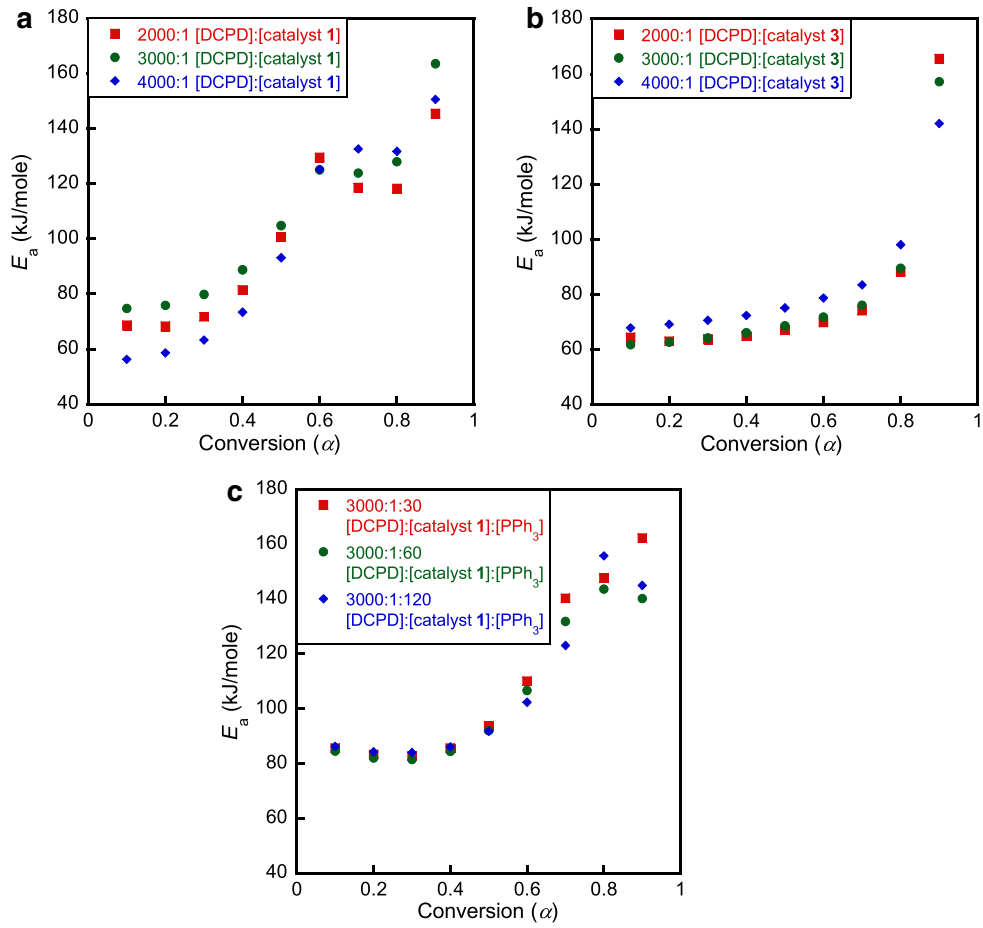

Fig. 8 Activation energy (E_a) profiles of **a** catalyst **1**, **b** catalyst **3**, and **c** catalyst **1** + PPh_3

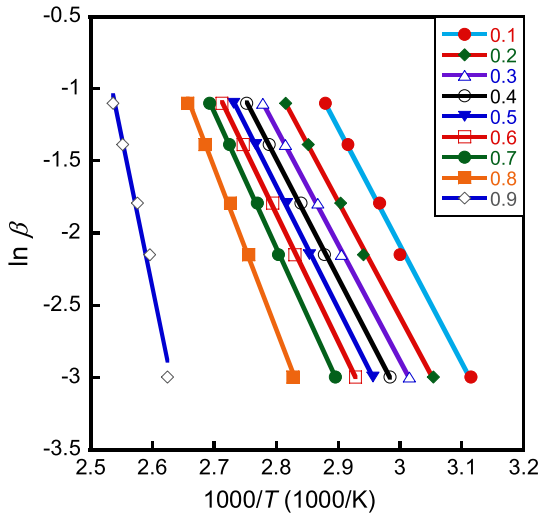

Fig. 9 A representative plot of ln β vs. $1/T_i$. Data presented here is taken from 2000:1 [DCPD]:[catalyst **3**]

coefficients (r^2) typically greater than 0.993 (a representative plot is shown in Fig. 9), so the deviations between Fig. 8a and b are not attributed to experimental error.

A hypothesis has been formulated to explain this result. It is assumed that since the activation energy in Fig. 8b remains fairly linear up to high conversions, followed by classic diffusion control, that heat evolved using catalyst **3** is solely a result of the ROMP reaction, while catalyst **1** undergoes one or more heat-evolving processes other than ROMP, thereby causing the deviations at conversions of $\alpha = 0.4$–0.8.

That the activation energy in Fig. 8a deviates from Fig. 8b only at middle-to-high conversions implies that whatever process may be occurring at $\alpha = 0.4$–0.8 is autocatalytic in nature. It is probably not truly autocatalytic in the sense that it does not help to propagate further polymerization (as evidenced by the lower T_g value for catalyst **1**), but instead initiates some other reaction on the polymer chain. This is consistent with the ΔH_{rxn} of catalyst **1** being about 30 J/g higher than with catalyst **3**, since this extra autocatalytic process would increase the heat evolved per unit mass.

This then leaves the question of what process besides ROMP could be evolving heat via reaction on the polymer chain, slightly reducing the T_g of the overall polymer, and why this process would occur with catalyst **1**, but not catalyst **3**. Highly active catalysts, including catalyst **1**, are

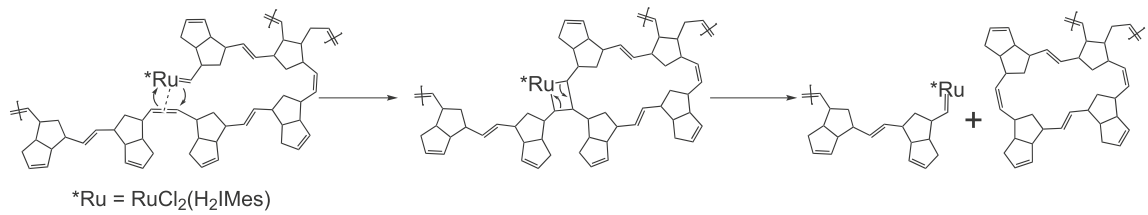

Fig. 10 An example of back biting on a pDCPD matrix

known to sometimes undergo cross-metathesis on the acyclic double bonds of the polymer chain, especially at high temperatures [23], in a process known as back biting, which could explain these results. An example of back biting on a pDCPD chain is shown in Fig. 10. This process is not nearly as exothermic as is the opening of a strained ring in ROMP, which explains why only a minor increase in ΔH_{rxn} is observed; it would cleave crosslinks on the polymer chain to leave either macrocyclic sidegroups or free molecules, which explains the drop in T_g; and the back biting would be most prominent at high degrees of cure where the amount of acyclic olefins are maximized, which explains why the anomalous peak does not occur at low conversions.

Back biting does not appear to be prominent in catalyst **3**, marked by a lack of an extra peak in Fig. 8b. When one turnover of ROMP is completed, the ruthenium catalyst exists as a 14-electron, 4-coordinate complex, shown as the last product in Fig. 3. A nearby sigma-donor, in the case of this study either olefin or phosphine, should quickly coordinate to this high energy, transient intermediate. If an olefin coordinates at high conversions where a large amount of acyclic double bonds are present, it is likely that the coordinating olefin will be acyclic, which means the back biting interaction would be favored. If instead phosphine coordinates, the catalyst is stabilized and, upon re-dissociation of that phosphine, can be more selective to undergo the more kinetically and thermodynamically favorable reaction with a cyclic monomer. It would then appear that the extent of back biting could potentially be related to the catalyst's relative binding affinity to olefin and phosphine. Both catalysts **1** and **3** should have equivalent binding affinities to olefin, since they are the same propagating metal center reacting with the same olefin monomer, but different binding affinities to their respective free phosphines, PCy_3 and PMe_3. Since binding affinity of a ligand to a substrate is typically inversely related to its rate of dissociation from that substrate [24], PMe_3 is expected to have a much higher binding affinity to its catalyst than PCy_3, and this higher affinity for phosphine in catalyst **3** would disfavor back biting reactions, relative to catalyst **1**.

Also lending evidence to this theory is the appearance of the anomalous peak occurring at high conversions in Fig. 8c. The free phosphine used here, PPh_3, is expected to have a much lower binding affinity to catalyst than either PCy_3 or PMe_3, as suggested by its low pKa (Table 2), and back biting reactions should be favored. However the binding affinity of PPh_3 to catalyst in these systems should effectively be higher than the pKa implies since such a large excess (30, 60, or 120 eq.) is present. This can potentially explain why the anomalous peak occurs at higher conversions for Fig. 8c than in Fig. 8a—a larger amount of acyclic double bonds, created at higher conversions, is necessary to statistically outweigh the increased amount of free phosphine.

Furthermore, with higher loadings of free phosphine to increase the effective binding affinity to catalyst, less back biting is expected to occur. This is corroborated by the ΔH_{rxn} decreasing with increasing phosphine loading.

Conclusions

In this study, several different ROMP-based catalytic systems were used to cure dicyclopentadiene, and the resulting curing behavior was analyzed by DSC. It was shown that, compared to the 2nd generation Grubbs' catalyst **1**, catalyst **3** was much more latent and is potentially useful to increase the pot-life of polymers made by ruthenium-based ROMP. Also, dicyclopentadiene cured with catalyst **1** + free phosphine had an increased latency over catalyst **1** alone, but with much higher activation energy and a much lower T_g. Reasons for the differences in latency, activation energy, ΔH_{rxn}, and glass transition temperature of all systems were discussed in detail.

Acknowledgements Financial support for this work was provided by the donors of The American Chemical Society Petroleum Research Fund (ACS PRF# 47700-AC7). We kindly thank Dr. Richard Larock for his donation of triphenylphosphine.

References

1. Ivin KJ, Mol JC. Olefin metathesis, metathesis polymerization. San Diego, CA: Academic Press; 1997.
2. Bielawski CW, Grubbs RH. Living ring-opening metathesis polymerization. Prog Polym Sci. 2007;32:1–29.
3. Grubbs RH, Tumas W. Polymer synthesis and organotransition metal chemistry. Science 1989;243:907–15.

4. Rouhi AM. Olefin metathesis: big-deal reaction. Chem Eng News. 2002;80:29–33.
5. Rouhi AM. Olefin metathesis: the early days. Chem Eng News. 2002;80:34–8.
6. Nguyen ST, Johnson LK, Grubbs RH. Ring-opening metathesis polymerization (ROMP) of norbornene by a group VIII carbene complex in protic media. J Am Chem Soc. 1992;114:3974–5.
7. Nguyen ST, Grubbs RH. Syntheses and activities of new single-component, ruthenium-based olefin metathesis catalysis. J Am Chem Soc. 1993;115:9858–9.
8. Dias EL, Nguyen ST, Grubbs RH. Well-defined ruthenium olefin metathesis catalysts: mechanism and activity. J Am Chem Soc. 1997;119:3887–97.
9. Grubbs RH. Olefin-metathesis catalysts for the preparation of molecules and materials. Angew Chem Int Ed. 2006;45:3760–5.
10. Scholl M, Ding S, Choon WL, Grubbs RH. Synthesis and activity of a new generation of ruthenium-based olefin metathesis catalysts coordinated with 1,3-dimesityl-4,5-dihydroimidazol-2-ylidene ligands. Org Lett. 1999;1:953–6.
11. Jones AS, Rule JD, Moore JS, White SR, Sottos NR. Catalyst morphology and dissolution kinetics for self-healing polymers. Chem Mater. 2006;18:1312–7.
12. Sanford MS, Love JA, Grubbs RH. A versatile precursor for the synthesis of new ruthenium olefin metathesis catalysts. Organometallics 2001;20:5314–8.
13. Bolton SL, Williams JE, Sponsler MB. Stablilization of (Trialkylphosphine)ruthenium alkylidene metathesis catalysts using phosphine exchange. Organometallics 2007;26:2485–7.
14. Ozawa T. A new method for analyzing thermogravimetric data. Bull Chem Soc Jpn. 1965;38:1881–6.
15. Flynn JH, Wall LA. A quick, direct method for the determination of activation energy from thermogravimetric data. Polym Lett. 1966;4:323–8.
16. Sanford MS, Love JA, Grubbs RH. Mechanism and activity of ruthenium olefin metathesis catalysis. J Am Chem Soc. 2001;123:6543–54.
17. Hong SH, Day MW, Grubbs RH. Decomposition of a key intermediate in ruthenium-catalyzed olefin metathesis reactions. J Am Chem Soc. 2004;126:7414–5.
18. Hong SH, Wenzel AG, Salguero TT, Day MW, Grubbs RH. Decomposition of ruthenium olefin metathesis catalysts. J Am Chem Soc. 2007;129:7961–8.
19. Metton® and Telene® brochures. Brochures downloaded from http://www.metton.com and http://www.telene.com.
20. Sanford MS, Ulman M, Grubbs RH. New insights into the mechanism of ruthenium-catalyzed olefin metathesis reactions. J Am Chem Soc. 2001;123:749–50.
21. Bielawski CW, Grubbs RH. Highly efficient ring-opening metathesis polymerization (ROMP) using new ruthenium catalysts containing N-heterocyclic carbene ligands. Angew Chem Int Ed. 2000;39:2903–6.
22. Kessler MR, White SR. Cure kinetics of the ring-opening metathesis polymerization of dicyclopentadiene. J Polym Sci Part A. 2002;40:2373–83.
23. Choi T-L, Grubbs RH. Controlled living ring-opening-metathesis polymerization by a fast-initiating ruthenium catalyst. Angew Chem Int Ed. 2003;42:1743–6.
24. Crabtree RH, editor. The organometallic chemistry of the transition metals. 4th ed. New York: John Wiley and Sons; 2005. p. 104–11.